

9. Carmona, N. B., Buatois, L. A. and Mángano, M. G., The trace fossil record of burrowing decapod crustaceans: evaluating evolutionary radiations and behavioural convergence. *Fossils Strata*, 2004, **51**, 141–153.
10. Mukhopadhyay, S. K., Trace fossils as palaeoenvironmental and sedimentological indices of coal-bearing Gondwana sequence. In Proceedings Volume IXth International Gondwana Symposium, New Delhi, India, 1996, vol. 1, pp. 248–254.
11. Gupta, A., Early Permian palaeoenvironment in Damodar Valley coalfields, India: an overview. *Gondwana Res.*, 1999, **2**, 149–165.
12. Bhattacharya, B. and Bhattacharya, H. N., Implications of trace fossil assemblages from late Paleozoic glaciomarine Talchir Formation, Raniganj Basin, India. *Gondwana Res.*, 2007, **12**, 509–524.
13. Bhattacharya, H. N. and Bhattacharya, B., Lithofacies architecture and palaeogeography of late Paleozoic glaciomarine Talchir Formation, Raniganj Basin, India. *J. Palaeogr.*, 2015, **4**(3), 40–55.
14. Chakraborty, A. and Bhattacharya, H. N., Ichnology of a Late Paleozoic (Permocarboniferous) glaciomarine deltaic environment, Talchir Formation, Saharjuri Basin, India. *Ichnos*, 2005, **12**(1), 31–45.
15. Bhattacharya, B. and Banerjee, S., Chondrites *isp.* Indicating late Paleozoic atmospheric anoxia in eastern peninsular India. *Sci. World J.*, 2014, **2014**, 1–9.
16. Bhattacharya, B., Bandyopadhyay, S., Mahapatra, S. and Banerjee, S., Record of tidewave influence on the coal-bearing Permian Barakar Formation, Raniganj Basin, India. *Sediment. Geol.*, 2012, **267–268**, 25–35.
17. Bhattacharya, B., Banerjee, S., Bhattacharjee, J. and Bandyopadhyay, S., Sedimentology and ichnology of Permian fluvio-marine Barakar Formation, Raniganj Basin, India. Abstr. vol. In 19th International Sedimentological Congress of the International Association of Sedimentologists (IAS-2014), Geneva, Switzerland, p. 72.
18. Bhattacharya, B. and Banerjee, P. P., Record of Permian Tethyan transgression in eastern India: a reappraisal of the Barren Measures Formation, West Bokaro Coalfield. *Mar. Petrol. Geol.*, 2015, **67**, 170–179.
19. Raja Rao, C. S. (ed.), Coal resources of Tamil Nadu, Andhra Pradesh, Orissa and Maharashtra. *Bull. Mem. Geol. Surv. India*, 1982, **45**(II), 41–52.
20. Tucker, M. E., *Sedimentary Petrology – An Introduction to the Origin of Sedimentary Rocks*, Blackwell Scientific Oxford, 1991, 2nd edn, p. 260.
21. Uchman, A. and Gaździcki, A., New trace fossils from the LaMeseta Formation (Eocene) of Seymour Island Antarctica. *Pol. Polar Res.*, 2006, **27**(2), 153–170.
22. Corner, J. D. and Fljåsted, A., Spreite trace fossils (*Teichichnus*) in a raised Holocene fjord-delta, Breidvikeidt, Norway. *Ichnos*, 1993, **2**, 155–164.
23. Fürsich, F. T., Trace fossils as environmental indicators in the Corallian of England and Normandy. *Lethaia*, 1975, **8**, 151–172.
24. Basan, P. B. and Scott, R. W., Morphology of *Rhizocorallium* and associated traces from the Lower Cretaceous Purgatoire Formation, Colorado. *Palaeogeogr. Palaeoclimatol. Palaeoecol.*, 1979, **28**, 5–23.
25. Knaust, D., The ichnogenus *Rhizocorallium*: classification, trace makers, palaeoenvironments and evolution. *Earth-Sci. Rev.*, 2013, **126**, 1–47.
26. Mukhopadhyay, G., Mukhopadhyay, S. K., Roychowdhury, M. and Parui, P. K., Stratigraphic correlation between different Gondwana Basins of India. *J. Geol. Soc. India*, 2010, **76**(3), 251–266.
27. Pemberton, S. G. and Frey, R. W., The *Glossifungites* ichnofacies: modern examples from the Georgia coast, USA. In *Biogenic Structures: Their Use in Interpreting Depositional Environments* (Curran, H. A. ed.), Society of Economic Paleontologists and Mineralogists (SEPM) Special Publication, 1985, vol. 35, pp. 237–259.
28. Gingras, M. K., Pemberton, S. G. and Saunders, T., Bathymetry, sediment texture and substrate cohesiveness: their impact on modern *Glossifungites* trace assemblages at Willappa Bay, Washington. *Palaeogeogr. Palaeoclimatol. Palaeoecol.*, 2001, **169**, 1–21.

ACKNOWLEDGEMENTS. B.B. thanks DST, New Delhi for funds through the DST FASTTRACK Research Project (No. SR/FTP/ES-170/2010). We thank the anonymous reviewers for constructive suggestions.

Received 10 November 2014; revised accepted 2 September 2015

doi:

Ascertaining the neotectonic activities in the southern part of Shillong Plateau through geomorphic parameters and remote sensing data

Watinaro Imsong¹, Swapnamita Choudhury¹ and Sarat Phukan^{2,*}

¹Wadia Institute of Himalayan Geology, Dehradun 248 001, India

²Department of Geological Sciences, Gauhati University, Guwahati 781 013, India

Study of quantitative morphometric parameters was taken up in four major river valleys in the southern part of Shillong Plateau using SRTM DEM in GIS. The study indicates that the region is undergoing differential uplift. This is evidenced by preferential tilting towards east, while the central part of the plateau exhibits higher rate of uplift than the eastern and western segments. We ascribed the higher rate of uplift in the central segment of Shillong Plateau to the activity along the Dapsi Thrust and Dauki Fault.

Keywords: Active tectonics, geomorphic parameters, morphometry, remote sensing, river basins.

THE Shillong Plateau is considered as a detached block of a subducted wedge of the peninsular India in front of the Indian and Tibetan continental mass¹. It is bounded by the Dauki Fault in the south, the Himalayan Orogenic Belt in the north, the Kopili Fault in the east and the Dhubri Fault in the west (Figure 1). Beyond the Dhubri Fault lies the Bengal Graben further to the south^{2–4}. The Shillong Plateau is considered as a tectonically active pop-up continental block^{1,5–8}. The existence of the proposed Oldham Fault⁷ (Figure 1) representing the northern margin of the pop-up tectonics is, however, debatable⁸. The Dauki Fault which runs along the border between the

*For correspondence. (e-mail: saratphukan@gmail.com)

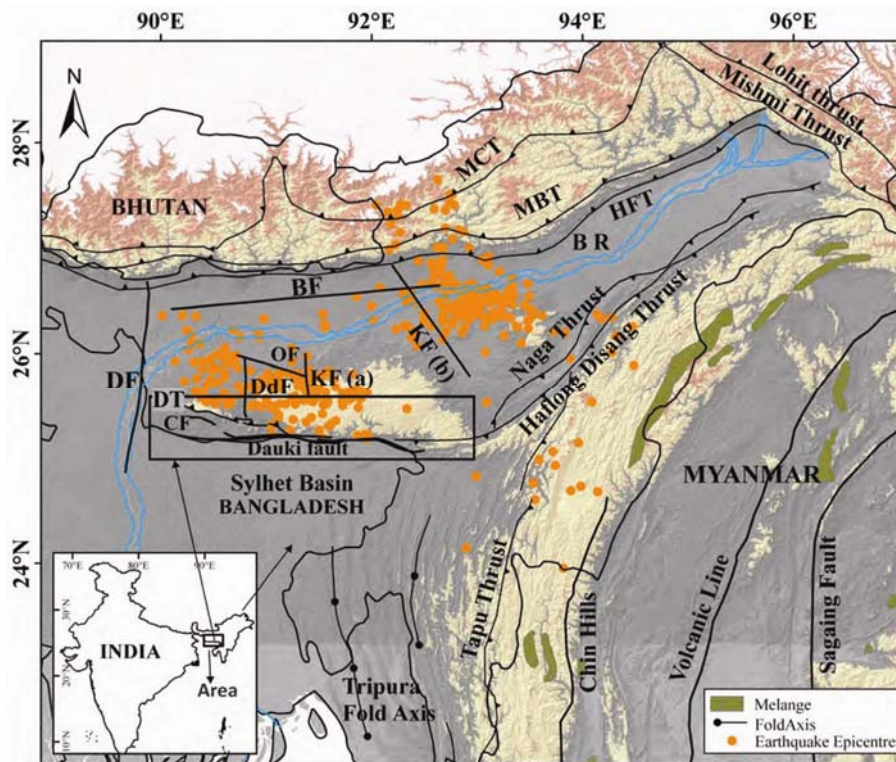


Figure 1. Shaded relief map of the Eastern Himalayan syntaxis along with the Shillong Plateau and the Sylhet Basin showing tectonic framework in and around the region. Earthquake epicentres USGS of the years 1973–2012. MCT, Main Central Thrust; MBT, Main Boundary Thrust; HFT, Himalayan Frontal Thrust; BF, Brahmaputra Fault; OF, Oldham Fault; DT, Dapsi Thrust; CF, Chokpot Fault; DF, Dhubri Fault; DdF, Dudnoi Fault; KF(a), Kulsu Fault and KF(b), Kopili Fault. The tectonic features have been marked with reference to Bilham and England⁷, Islam *et al.*²⁷, Biswas and Grasemann²⁸ and satellite images.

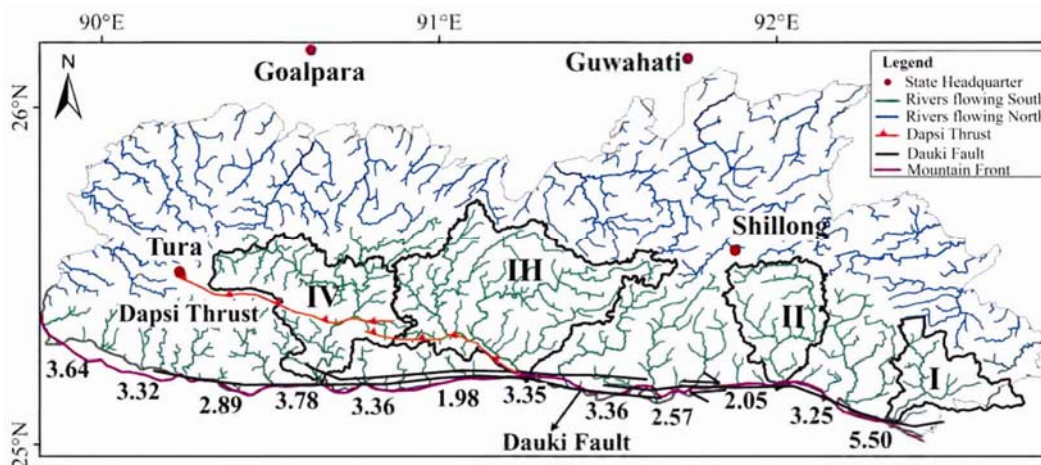


Figure 2. Drainage map of the study area and location of the four river basins investigated in the present study. The basins are from east to west: (I) Lubha River Basin, (II) Umngot River Basin, (III) Jadukata River Basin and (IV) Simsang River Basin. The mountain front sinuosity along the southern periphery of the plateau is also shown.

Shillong Plateau and the Sylhet Basin of Bangladesh, marks a spectacular topographic discordance in the region. Along this fault the general elevation difference of the Shillong Plateau and the Sylhet Basin is around 500–700 m in the central part of the plateau. The Pre-

cambrian basement in the Sylhet Basin of Bangladesh is located at ~ 18 km, and is exposed at places a few hundred metres below the surface, particularly along the southern fringe of the plateau. Thus, it represents an active plateau margin. Based on GPS survey, Banerjee

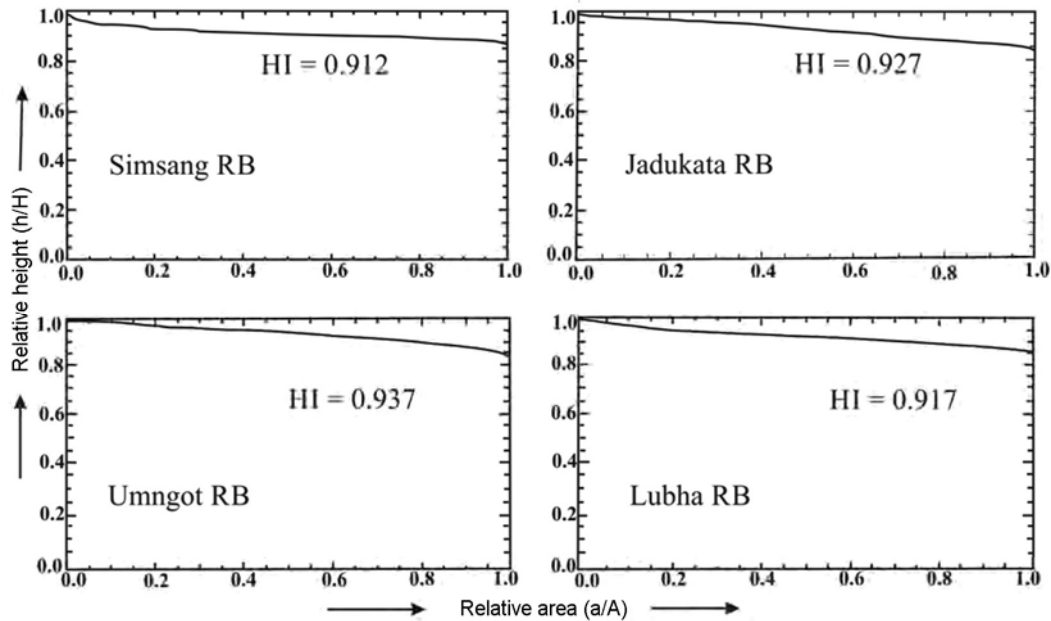


Figure 3. Percentage hypsometric curve of the selected river basins. The calculated HI index gives very high values and the hypsometric curves are straight to convex upward which indicates young and uplifting topography.

*et al.*⁹ suggested that the eastern segment of the Indian plate shows rapid shortening and higher convergent rates compared to the rest of the plate.

Tectonic behaviour of the Shillong Plateau is believed to be diverse in different segments. Chatterjee *et al.*¹⁰ postulated two tectonic domains in the Shillong Plateau with occurrence of the Prydz Bay Suture possibly between the Garo–Goalpara Hills and Sonapahar areas. Duarah and Phukan¹ identified relatively young landforms in the central part compared to deeply eroded eastern and western parts. They also showed varied tectonic fabrics in the eastern and western segments of the plateau. The western part shows NE–SE trending structural elements, whereas in the eastern part there is a prominent N–S trend.

Considering the tectonic configuration, it is expected that the drainage basins should respond to the cumulative expression of the tectonic activity in the plateau. In view of this, we selected four basins which drain towards the southern boundary across the Dauki Fault. These are from east to west (i) Lubha River Basin, (ii) Umngot River Basin, (iii) Jadukata River Basin and (iv) Simsang River Basin (Figure 2).

The Lubha River Basin is triangular-shaped and situated at the easternmost part of Meghalaya in the Jaintia Hills district, having a total drainage area of 647 sq. km. The Umngot River Basin falls in the Jaintia Hills and East Khasi Hills districts with an area of 872 sq. km. The Jadukata is the biggest river basin in Meghalaya and falls in the central part of the plateau in the West Khasi Hills district covering an area of 2455 sq. km. The Simsang River Basin falls in the South and West Garo Hills districts. It has a total drainage area of 1458 sq. km and

shares its eastern boundary with the Jadukata River Basin.

The Shillong Plateau represents a central upland, surrounded by highly dissected hills in the northern, eastern and mid-western parts, and also a narrow alluvial tract along the western border, flat-topped topography in the middle part, and deep gorges associated along the southern fringe. The general elevation ranges from about 15 m along its western boundary with Bangladesh, to 1966 m in the Shillong Peak in the central upland.

Based on the drainage pattern, it can be suggested that the sub-surface structures in the region control the drainage pattern. The plateau is almost equally halved by the drainage divide between north-flowing and south-flowing rivers (Figure 2). The south-flowing rivers form deep gorges along the southern periphery of the plateau as a result of massive headward erosion by these antecedent rivers, which is ascribed to the rapid upliftment of the plateau¹¹.

The plateau is an old cratonic block which is dominantly composed of rocks of Precambrian age. It is devoid of any rock sequence that had been deposited during the period from Neo-Proterozoic to early Cretaceous. During the early Cretaceous fracturing of the plateau and extrusion of lavas of the Sylhet Trap transpired, which is genetically related to the Keruguelen hotspot of the Indian Ocean¹². Following this, the region witnessed a transgressive phase, particularly along the southern fringe of the plateau that led to the deposition of sediment belonging to the Upper Cretaceous to Cenozoic.

The basins investigated in the present study largely drain through the Precambrian rocks in the northern parts and the Upper Cretaceous–Cenozoic sedimentary cover

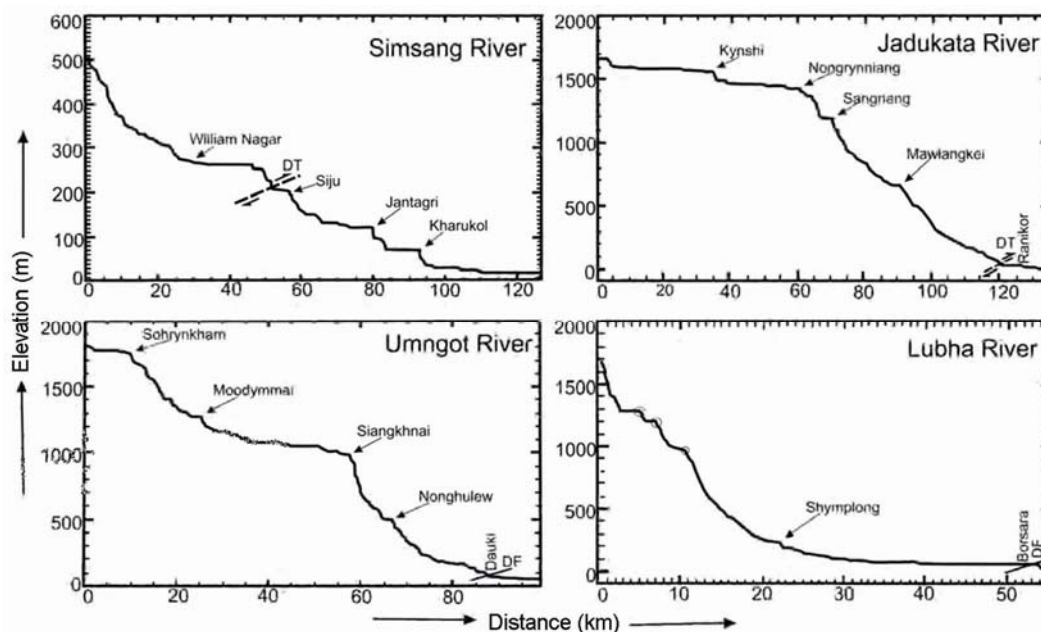


Figure 4. Longitudinal profiles of the longest channel of each of the river basins showing a number of knick points as well as the position of Dapsi Thrust and Dauki Fault along the channel.

along the southern fringe of the plateau. The Dauki Fault runs along the southern boundary of the plateau, beyond which the rivers enter the Bangladesh plain. The Dapsi Thrust passes through the middle of the Simsang River Basin with WNW–ESE strike and meets the Dauki Fault near the Jadukata river course (Figure 2).

Earthquake data from USGS show high concentration of seismic activity within the central, western and north-western parts of the plateau (Figure 1), suggesting the tectonically active nature of the terrain. Further, aeromagnetic data show the presence of major discontinuities such as faults, fractures and shears¹³. Based on the surficial expressions through satellite images and digital elevation models of the plateau, it can be suggested that the Dapsi Thrust which merges with the Dauki Fault is undergoing enhanced tectonic deformation (Figure 1). Flexure of the north-verging thrust can be seen in the outcrops at Dauki in the field.

Clark and Bilham¹⁴ suggested that deformation of the Shillong Plateau was initiated in the mid to late Miocene. Earthquake epicentres also show that the central part of the plateau is tectonically active followed by its western part, while the eastern part shows relatively less activity. This is ascribed to the clockwise rotation of the plateau¹⁵, which is also supported by a GPS study⁹. From geological, archaeological and historical data Rajendran *et al.*⁸ suggested recurrence of large earthquakes in 1200 years and contradicted 3000–8000 years of recurrence intervals as suggested by Bilham and England⁷.

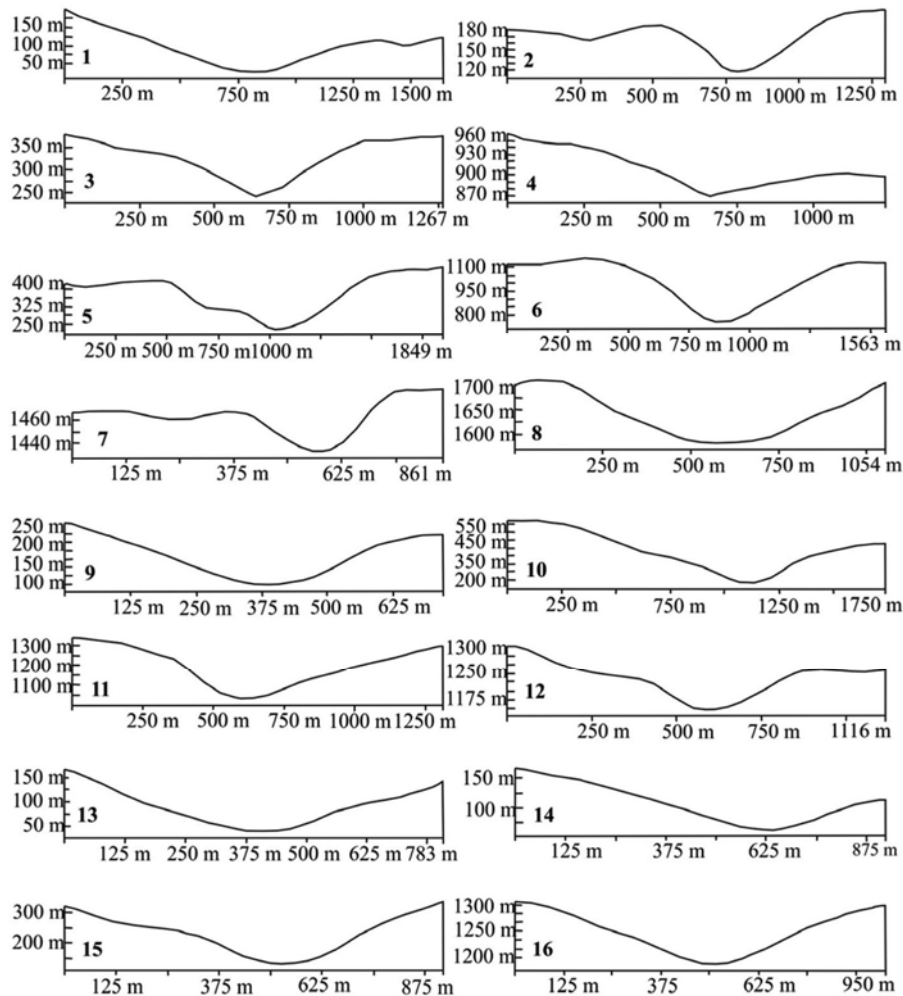
The present study is based on analysis of remote sensing data on GIS platform using RiverTools 3.0 and ArcGIS 9, along with SRTM DEM of ~90 m resolution.

The SRTM mission was flown in February 2000 and provides a topography covering continental areas from 60°N to 56°S (ref. 16). The mission generated two digital elevation models at 1 and 3 arcsec spatial resolution (~30 and ~90 m resolution respectively). The SRTM DEM (v.2) is used in the ‘River Tool’ software for extracting drainage network and its properties. For extracting the drainage network, the ‘strahler order’ method was followed¹⁷; the pruning threshold was taken as 3, since it yielded the best results¹⁸.

Relief is a function of tectonics and erosion. Thus, in a river basin with varying tectonics, the uplifted area would have more relief than the tectonically less-affected areas and can be assessed using hypsometric curve and hypsometric integral (HI) of Strahler¹⁷. HI is a dimensionless character and can be utilized to compare different catchments irrespective of scale¹⁹. It integrates three dimensions, combining area on the x -axis with elevation on the y -axis. This can be used as a measure of the erosional state or geomorphic age of the catchment and is considered as a powerful tool for differentiating tectonically active regions from inactive ones¹⁹. In theory, hypsometric integral value ranges from 0 to 1. Low values are interpreted to represent old eroded landscapes, and high values as young, less-eroded landscapes. Pike and Wilson²⁰ demonstrated mathematically that the elevation/relief ratio (E) (which is defined as $E = (\text{mean elevation} - \text{minimum elevation}) / (\text{maximum elevation} - \text{minimum elevation})$) is identical to HI, but has the advantage that it is much easier to obtain numerically. The hypsometric curve produced is essentially a frequency distribution of elevations in a given area. A convex-up curve means that

Table 1. Parameters calculated from longitudinal profile of the longest channel of the given rivers using River Tools 3.0

River basin	Total reach length (km)	Average elevation drop (m)	Reach slope (m/m)	Average sinuosity (m/m)
Simsang	125	2.49	2.565	2.308
Jadukata	135	2.17	4.714	1.36
Umngot	98	1.09	1.691	1.73
Lubha	55	7.20	4.64	1.19

**Figure 5.** Valley profiles 1–4 represent Simsang River, 5–8 represent Jadukata River, 9–12 represent Umngot River, and 13–16 represent Lubha River. The profiles 2, 3, 5–7, 10–12 and 15 show asymmetric tilting (on the right).

most of the area has relatively enhanced uplift with low erosion. A concave-up curve means that most of the area has relatively less uplift and high erosion.

In case of the selected river basins, hypsometric curves are straight to gently convex upward (Figure 3), which represents very young topography. The HIs of the selected river basins range from 0.912 to 0.937. This indicates that the entire Shillong Plateau is undergoing uplift in the recent geological time.

According to Gilbert²¹, the slope of a longitudinal profile is inversely proportional to the discharge. Radoane *et al.*²² showed that the type of riverbed material, sediment discharge and the nature of bedrock have a major influence on the stream bed profile. The stream geometry of a longitudinal profile allows us to infer the underlying material, geologic processes, geomorphic history and neotectonic activities of an area¹⁵. The longitudinal profile of the longest channel of sixth order Simsang River,

eighth order Jadukata River, seventh order Umngot River and eighth order Lubha River shows a number of knick points (Figure 4). All the four rivers show steeper slopes in their middle segment followed by gentler slopes in the lower segment. Elements such as total reach length, average sinuosity, reach slope and average elevation drop of all the four rivers have been extracted from the longitudinal profile using River Tools 3.0 (Table 1).

The longitudinal profiles indicate that the bedrock erosion is higher in Simsang and Lubha rivers compared to the Jadukata and Umngot rivers. This can be ascribed to enhanced surface (bedrock) uplift and juvenile nature of the terrain in the central part of the plateau.

Tilting of valleys or asymmetrical valley slopes can be attributed to the tectonically active nature of the terrain, or alternatively, it may be caused due to varying geologic, hydrologic or climatic conditions^{15,23}. Normally, the upper reaches of a river would show steep valley profiles and the lower reaches would show gentler and wider valley profiles^{24,25}. The Simsang River valley profiles show steep valleys in the middle course of the river channel while the lower course of the Jadukata River is steeper compared to the upper course. The Umngot and Lubha River profiles show flatter valleys indicative of mature terrain. In Figure 5, the profile sections along 2, 3, 5–7, 10–12 and 15 show asymmetric tilting on the right side of the bank. This can be caused by preferential (towards left) tilting of the river catchment.

The basin asymmetry factor (AF) can be used to detect tectonic tilting in drainage basins. $AF = 100 (A_r/A_t)$, where A_r is the area of the basin to the right (facing downstream) of the trunk stream, and A_t is the total area of the drainage basin. A value of AF greater or less than 50 may suggest tilting. If AF is >50 , it implies tilt down to the left basin (looking downstream), and if tilting is to the right basin, AF would be <50 (ref. 24). Figure 6 shows the river basins with their longest streams. Table 2 gives the AF of the river basins.

The Simsang River Basin shows marginal tilt towards the left, whereas the Jadukata, Umngot and Lubha River Basins show an appreciable tilt towards the right flank of the basin/towards eastern side of the plateau.

The mountain front sinuosity (S_{mf}) reflects the balance between erosional forces (that tend to cut embayment into a mountain front) and the tectonic forces that tend to produce a straight front coincident with any active range-bounding $S_{mf} = L_{mf}/L_s$, where L_{mf} is the length of the mountain front along the mountain–piedmont (foot of the mountain) junction, and L_s is the straight-line length of the mountain front. Mountain fronts associated with active tectonics and uplift are straight and have low values of S_{mf} (refs 24, 25). The S_{mf} values calculated are lowest in the central, mid-eastern and mid-western segments, which indicates that these are more active than the other segments. Table 3 shows the mountain front sinuosity on the southern front of the plateau and Figure 2

shows the extent of the S_{mf} measured at different segments.

Quantitative analysis of four major river basins in the southern front of the Shillong Plateau, namely; Simsang, Jadukata, Umngot and Lubha River Basins indicates young topography in all of them. Morphometric indices suggest that the part of the plateau under study is undergoing crustal deformation, and incision and uplift seem to be in equilibrium. The hypsometric curves and indices of

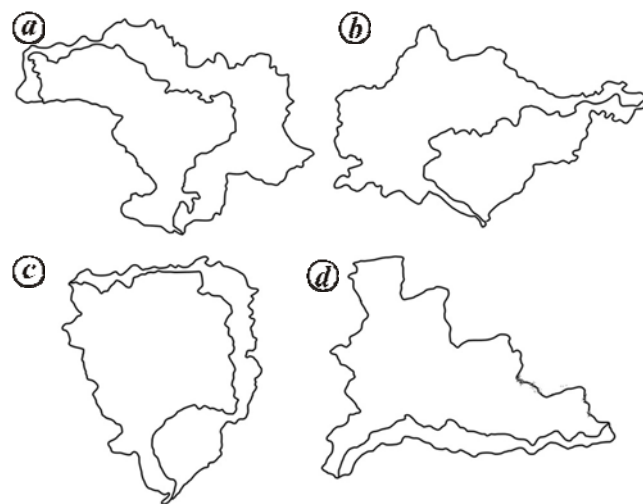


Figure 6. Asymmetric tilting of the four river basins as indicated by the longest channel in the basin. *a*, Simsang River Basin; *b*, Jadukata River Basin; *c*, Umngot River Basin; *d*, Lubha River Basin.

Table 2. Calculated asymmetry factor (AF) for the given river basins

River basin	AF
Simsang	50.35
Jadukata	35.32
Umngot	29.77
Lubha	14.82

Table 3. Mountain front sinuosity on the southern front of the Shillong Plateau

Extent	S_{mf}
89°49'34.95"E–89°59'21.67"E	3.64
89°59'25.73"E–90°12'41.05"E	3.32
90°12'42.55"E–90°26'31.26"E	2.89
90°26'31.94"E–90°40'41.72"E	3.78
90°40'44.23"E–90°54'21.81"E	3.36
90°54'22.29"E–90°8'57.96"E	1.98
91°8'58.45"E–91°23'18.24"E	3.35
91°23'9.06"E–91°37'26.70"E	3.36
91°37'27.09"E–91°50'35.97"E	2.57
91°50'36.26"E–92°5'13.31"E	2.05
92°5'14.38"E–92°17'42.20"E	3.25
92°17'42.19"E–92°26'43.21"E	5.50

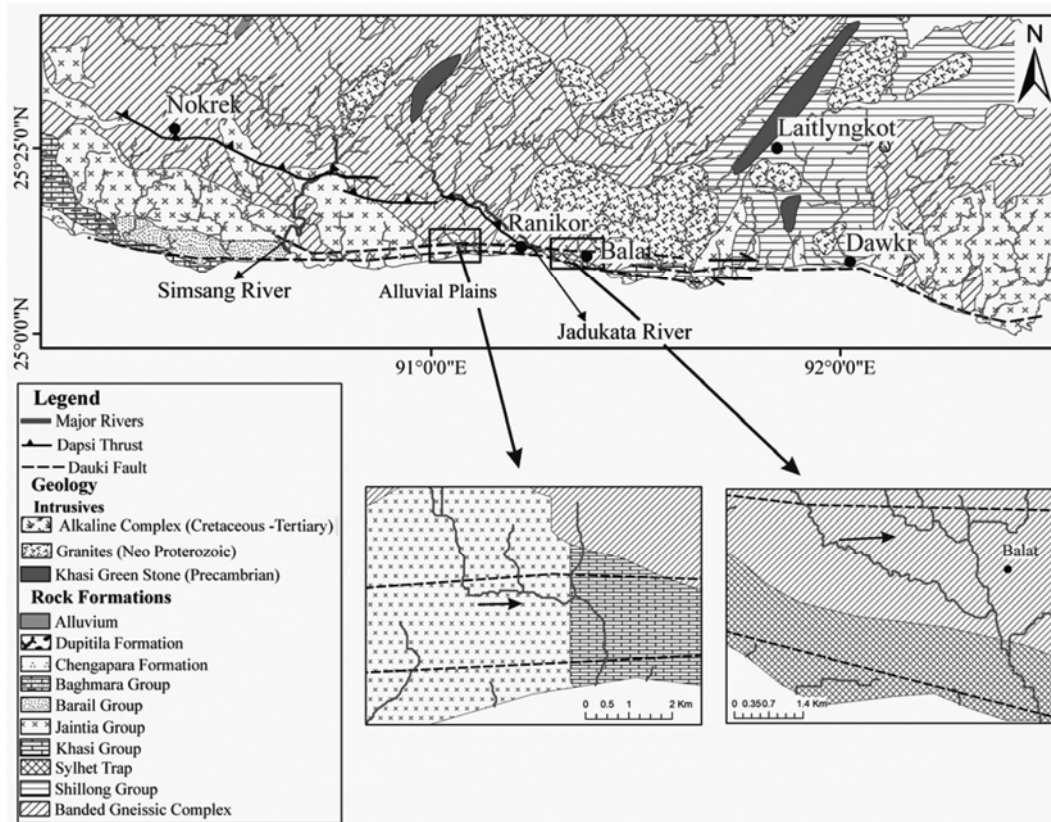


Figure 7. Small river channels showing right lateral deflection in the central section of the southern periphery of the Shillong Plateau.

the river basins demonstrate similar configurations and values, and indicate that the entire plateau is undergoing uplift. However, the longitudinal profiles of the Simsang River (western segment) and the Lubha River (eastern segment) are found to be more eroded than the Jadukata and Umngot Rivers, which are present in the central part of the plateau. Major knick points in all the river channels show prominent topographic breaks. The Dapsi Thrust is traversed by the Simsang River in its middle reach and meets Jadukata River in its lower reach near the interface of the Dauki Fault. This may be the cause of the presence of steeper courses in the middle reach of the Simsang River and lower reach of the Jadukata River, implying structural control on river morphology. This is further supported by the low river sinuosity values of the longest channel of all the river basins, which indicates that the channels are structurally controlled (Table 1). Additionally, numerous small channels (third and fourth order streams) around the central section on the southern periphery of the plateau show right lateral deflection in the river course. These accord well with the sense of movement associated with the Dauki Fault (Figure 7). Figure 7 shows the deflection of (third and fourth order) streams towards the east.

The higher surface uplift of the central part of the plateau compared to the western and eastern parts is also

reflected in the analysis of mountain front sinuosity. S_{mf} of the eastern part of the plateau is found to be the highest, which is associated with less activity. The basin asymmetric factor of Simsang River shows slight tilt towards the west, whereas the Jadukata, Umngot and Lubha River Basins show obvious tilting towards the east. This may be suggestive of the presence of two different tectonic domains in the eastern and western parts of the Shillong Plateau (Garo-Goalpara region) as suggested by Chatterjee *et al.*¹⁰. Although preliminary in nature, the present study suggests that the entire Shillong Plateau is undergoing tectonic instability, but, the central segment of the plateau is witnessing accelerated deformation/uplift. Further, the study indicates that the observed deformation in the river basins is associated with the episodic activity along the Dapsi Thrust and the Dauki Fault.

1. Duarah, B. P. and Phukan, S., Understanding the tectonic behavior of Shillong Plateau, India using Remote Sensing Data. *J. Geol. Soc. India*, 2011, **77**, 105–112.
2. Angelier, J. and Baruah, S., Seismotectonics in Northeast India: a stress analysis of focal mechanism solutions of earthquakes and its kinematic implications. *Geophys. J. Int.*, 2001, **178**, 303–326.
3. Evans, P., The tectonic framework of Assam. *J. Geol. Soc. India*, 1964, **5**, 80–96.
4. Nandy, D. R., *Geodynamics of Northeastern India and the Adjoining Region*, ACB Publication, Kolkata, 2001, p. 209.

5. Kayal, J. R., Seismicity of northeast India and surroundings, development over the past 100 years. *J. Geophys.*, 1998, **19**, 9–34.
6. Nandy, D. R., Tectonic evolution of north-eastern India and adjoining area with special emphasis on contemporary geodynamics. *Indian J. Geol.*, 2000, **72**(3), 175–195.
7. Bilham, R. and England, P., Plateau pop-up during the great 1897 Assam earthquake. *Nature*, 2001, **410**, 806–809.
8. Rajendran, C. P., Rajendran, K., Duarah, B. P., Baruah, S. and Earnest, A., Interpreting the style of faulting and paleoseismicity associated with the 1897 Shillong, northeast India, earthquake: implications for regional tectonism. *Tectonics*, 2004, **23**(4), 1–12.
9. Banerjee, P., Burgmann, R., Nagarajan, B. and Apel, E., Intraplate deformation of the Indian subcontinent. *Geophys. Res. Lett.*, 2008, **35**, L18301, 1–5.
10. Chatterjee, N., Mazumdar, A. C., Bhattacharya, A. and Saikia, R. R., Mesoproterozoic granulites of the Shillong–Meghalaya Plateau: evidence of westward continuation of the Prydz Bay Pan-African suture into Northeastern India. *Precambrian Res.*, 2007, **152**, 1–26.
11. Soil and Water Conservation Department, Government of Meghalaya. http://megsoil.gov.in/basic_inf.htm
12. Ghatak, A. and Basu, A. R., Vestiges of the Kerguelen Plume in the Sylhet Traps, northeastern India. *Earth Planet. Sci. Lett.*, 2011, **308**, 52–64.
13. Sharma, R., Gouda, H. C., Singh, R. K. and Nagaraju, B. V., Structural study of Meghalaya Plateau through aeromagnetic data. *J. Geol. Soc. India*, 2012, **79**, 11–29.
14. Clark, M. K. and Bilham, R., Miocene rise of the Shillong Plateau and the beginning of the end for the Eastern Himalaya. *Earth Planet. Sci. Lett.*, 2008, **269**, 336–350.
15. Duarah, B. P. and Phukan, S., Seismic hazard assessment in the Jia Bhareli river catchment in eastern Himalaya from SRTM-derived basin parameters, India. *Nat. Hazards*, 2011, **59**, 367–381.
16. Rabus, B., Eineder, M., Roth, A. and Bamler, R., The Shuttle Radar Topography Mission – a new class of digital elevation models acquired by space borne radar. *ISPRS J. Photogramm. Remote Sensing*, 2003, **57**, 241–262.
17. Strahler, A. N., Hypsometric (area–altitude) analysis of erosional topography. *GSA Bull.*, 1952, **63**, 1117–1142.
18. Rivix, River Tools (topographic and river network analysis) version 3.0, User's guide, 2005.
19. Dowling, T. I., Richardson, D. P., O'Sullivan, A., Summerell, G. K. and Walker, I., Application of hypsometric integral and other terrain based matrices as indicators of the catchment health: a preliminary analysis. CSIRO Land and Water, Technical Report 20/98, 1998.
20. Pike, R. J. and Wilson, S. E., Elevation–relief ratio, hypsometric integral and geomorphic area–altitude analysis. *Geol. Soc. Am. Bull.*, 1971, **82**, 1079–1084.
21. Gilbert, G. K., Report on the Geology of Henry Mountains. US Geographical and geological survey of the rocky mts region US Government Printing Office, Washington, DC, 1877.
22. Radoane, M., Radoane, N. and Dumitriu, D., Geomorphological evolution of longitudinal river profiles in the Carpathians. *Geomorphology*, 2002, **50**, 293–306.
23. Roy, S. S., A new approach to the analysis of transverse river valley profiles and implications for morph tectonics: a case study in Rajasthan. *Curr. Sci.*, 2001, **81**(1), 106–112.
24. Keller, E. A. and Pinter, N., *Active Tectonics: Earthquake, Uplift, and Landscape*, Prentice Hall, NJ, USA, 2002, 2nd edn, pp. 121–147.
25. Goudie, A. S., *Encyclopedia of Geomorphology*, Routledge Ltd, 2004, p. 1036.
26. Islam, M. S., Shinjo, R. and Kayal, J. R., Pop-up tectonics of the Shillong Plateau in northeastern India: insight from numerical simulations. *Gondwana Res.*, 2011; doi: 10.1016/j.gr.2010.11.007.
27. Biswas, S. and Grasemann, B., Quantitative morphotectonics of the southern Shillong Plateau (Bangladesh/India). *Aust. J. Earth Sci.*, 2005, **97**, 82–93.
28. Bull, W. B. and McFadden, L. D., Tectonic geomorphology north and south of the Garlock fault, California. In *Geomorphology in Arid Regions: Proceedings, Eight Annual Geomorphology Symposium* (ed. Doehring, D. O.), SUNY Binghamton, NY, USA, 1977, pp. 115–138.

ACKNOWLEDGEMENTS. We thank Dr B. P. Duarah, Head, Department of Geological Sciences, Gauhati University, and the Director, Wadia Institute of Himalayan Geology, Dehradun for providing the necessary facilities. W.I. thanks the Council of Scientific and Industrial Research, New Delhi for Junior Research Fellowship.

Received 19 November 2014; revised accepted 7 April 2015

doi: